

MOL Manuscript # 14258

## Altered Expression of $G_{q/11}\alpha$ Protein Shapes mGlu1 and mGlu5 Receptor-mediated Single Cell Inositol 1,4,5-trisphosphate and $Ca^{2+}$ Signaling

Peter J. Atkinson, Kenneth W. Young, Steven J. Ennion, James N.C. Kew, Stefan R. Nahorski, and R. A. John Challiss

*Department of Cell Physiology & Pharmacology (P.J.A., K.W.Y., S.J.E., S.R.N., R.A.J.C), University of Leicester, Maurice Shock Medical Sciences Building, University Road, Leicester, LE1 9HN, United Kingdom; and Psychiatry Centre of Excellence for Drug Discovery (J.N.C.K), GlaxoSmithKline, Harlow, CM19 5AW, United Kingdom*

MOL Manuscript # 14258

**Running Title:** G<sub>q/11</sub>α expression and IP<sub>3</sub> and Ca<sup>2+</sup> signaling

**Address for correspondence:** Prof. R.A.J. Challiss, Department of Cell Physiology & Pharmacology, University of Leicester, Maurice Shock Medical Sciences Building, University Road, Leicester, LE1 9HN, U.K.

Tel.: +44-116-252-2920

Fax: +44-116-252-5045

Email: [jc36@le.ac.uk](mailto:jc36@le.ac.uk)

Manuscript pages:	<b>27 (+ 8 figure pages)</b>
Tables:	<b>1</b>
Figures:	<b>8</b>
References:	<b>40</b>
Words in Abstract:	<b>246</b>
Words in Introduction:	<b>745</b>
Words in Discussion:	<b>1434</b>

**ABBREVIATIONS:** IP<sub>3</sub>, inositol 1,4,5-trisphosphate; GPCR, G protein-coupled receptor; eGFP-PH<sub>PLCδ</sub>, PH domain of PLCδ1 tagged with enhanced green fluorescent protein; CHO, Chinese hamster ovary; HEK, human embryonic kidney; mACh, muscarinic acetylcholine; mGlu, metabotropic glutamate; CICR, Ca<sup>2+</sup>-induced Ca<sup>2+</sup>-release.

## ABSTRACT

The metabotropic glutamate (mGlu) receptors, mGlu1 and mGlu5, mediate distinct inositol 1,4,5-trisphosphate (IP<sub>3</sub>) and Ca<sup>2+</sup> signaling patterns, governed in part by differential mechanisms of feedback regulation following activation. Single cell imaging has previously shown that mGlu1 receptors initiate sustained elevations in IP<sub>3</sub> and Ca<sup>2+</sup>, which are sensitive to agonist concentration. In contrast, mGlu5 receptors are subject to cyclical PKC-dependent uncoupling and consequently mediate co-incident IP<sub>3</sub> and Ca<sup>2+</sup> oscillations that are largely agonist concentration-independent. Here, we have investigated the contribution of G<sub>q/11</sub>α protein expression levels in shaping mGlu1/5 receptor-mediated IP<sub>3</sub> and Ca<sup>2+</sup> signals, using RNA interference (RNAi). RNAi-mediated knockdown of G<sub>q/11</sub>α almost abolished the single-cell increase in IP<sub>3</sub> caused by mGlu1 and mGlu5 receptor activation. For the mGlu1 receptor, this unmasked base-line Ca<sup>2+</sup> oscillations that persisted even at maximal agonist concentrations. mGlu5 receptor-activated Ca<sup>2+</sup> oscillations were still observed, but were only initiated at high agonist concentrations. Recombinant over-expression of G<sub>q</sub>α enhanced IP<sub>3</sub> signals following mGlu1 and mGlu5 receptor activation. Interestingly, although mGlu5 receptor-mediated IP<sub>3</sub> and Ca<sup>2+</sup> oscillations in control cells were largely insensitive to agonist concentration, increasing G<sub>q</sub>α expression converted these oscillatory signatures to sustained plateau responses in a high proportion of cells. In addition to modulating temporal Ca<sup>2+</sup> signals, up- or down-regulation of G<sub>q/11</sub>α expression alters the threshold for the concentration of glutamate at which a measurable Ca<sup>2+</sup> signal could be detected. These experiments indicate that altering G<sub>q/11</sub>α expression levels differentially affects spatio-temporal aspects of IP<sub>3</sub> and Ca<sup>2+</sup> signaling mediated by the mGlu1 and mGlu5 receptors.

## Introduction

Activation of the phospholipase C (PLC) pathway via coupling of G protein-coupled receptors (GPCRs) to guanine nucleotide-binding proteins (G proteins) of the  $G_{q/11}$  family results in inositol 1,4,5-trisphosphate ( $IP_3$ ) production and mobilization of intracellular calcium ( $Ca^{2+}$ ). Receptor activation can initiate spatially and temporally unique  $Ca^{2+}$  signals and thereby regulate an array of cellular processes (Berridge et al., 2000). Here, we have investigated the contribution of  $G_{q/11}\alpha$  protein expression in shaping receptor-initiated  $IP_3$  and  $Ca^{2+}$  signaling patterns.

The group I metabotropic glutamate receptors, mGlu1a and mGlu5a, are family C GPCRs. mGlu1a and mGlu5a receptors couple preferentially to the major isoforms of the  $G_q$  family,  $G_q\alpha$  and  $G_{11}\alpha$ , and are capable of activating distinct patterns of  $Ca^{2+}$  mobilization (Hermans and Challiss, 2001). Stimulation of the mGlu1a receptor predominantly initiates a peak-and-plateau  $Ca^{2+}$  response, whilst mGlu5a receptor activation mediates a  $Ca^{2+}$  oscillatory response over a broad range of stimulus-strengths (Nash et al., 2002). Previous studies proposed that mGlu5 receptor-mediated  $Ca^{2+}$  oscillations occur due to feedback inhibition via PKC-dependent phosphorylation of a single threonine (Thr<sup>840</sup>) residue (Kawabata et al., 1996), however very recent studies have shown that Thr<sup>840</sup> is not phosphorylated, but instead plays a structural/permissive role for the phosphorylation of an adjacent (Ser<sup>839</sup>) residue by PKC (Kim et al., 2005). Similar PKC-dependent  $Ca^{2+}$  oscillations have also been described following glutamate activation of astrocytes (Codazzi et al., 2001) and activation of another family C GPCR, the  $Ca^{2+}$ -sensing receptor (Young et al., 2002). Use of the pleckstrin homology (PH) domain of phospholipase C $\delta$  tagged with enhanced green fluorescent protein (eGFP-PH<sub>PLC $\delta$</sub> ) has enabled  $IP_3$  oscillations underlying mGlu5a receptor-activated  $Ca^{2+}$  oscillations to be observed (Nash et al., 2001, 2002; Nahorski et al., 2003). These PKC-dependent  $Ca^{2+}$  oscillations (referred to as “dynamic uncoupling”) are distinct from regenerative  $Ca^{2+}$ -induced  $Ca^{2+}$ -release (CICR), which is generated through an intrinsic property of the  $IP_3$  receptor (Thomas et al., 1996; Taylor and Thorn, 2001). CICR oscillations can be maintained with a relatively low steady-state increase in  $IP_3$ , as observed following activation of the  $M_3$  muscarinic acetylcholine (mACh) receptor with a low agonist concentration in the same cell background (Nash et al., 2001). Our previous studies exploring the determinants of mGlu5 receptor signaling led us to propose a model in which  $Ca^{2+}$  oscillation frequency is dependent on receptor expression levels, but is largely independent of agonist concentration (Nash et al., 2002). However, the importance of receptor-G protein coupling efficiency in group I mGlu

receptor-mediated  $\text{Ca}^{2+}$  signaling has not been investigated to date. Clearly, regulation and localization of  $\text{G}_{q/11}\alpha$  proteins could be a key, influencing factor in shaping the  $\text{Ca}^{2+}$  signals produced.

Studies examining the role of  $\text{G}_{q/11}\alpha$  proteins generally, and in conjunction with mGlu receptor signaling, have been facilitated greatly by the generation of  $\text{G}_{q/11}\alpha$  knockout mice (see Offermanns, 2003 for review]. However, gene deletion studies are limited by the mortality of  $\text{G}_q\alpha/\text{G}_{11}\alpha$  double-knockout mice, and also by the possibility that the phenotype of the cells studied may adapt to compensate for the loss of a particular  $\text{G}\alpha$ , as observed for the deletion of other G protein subtypes, including  $\text{G}_o\alpha$  (Greif et al., 2000) and  $\text{G}_{15}\alpha$  (Davignon et al., 2000). Other investigators have successfully used antisense methods to reduce  $\text{G}_{q/11}\alpha$  expression, however, often these studies rely on microinjection, making an accurate determination of endogenous  $\text{G}_q\alpha$  and  $\text{G}_{11}\alpha$  protein expression difficult to ascertain (Macrez-Lepretre et al., 1997; Haley et al., 1998). Determining the relative  $\text{G}_q\alpha$  and  $\text{G}_{11}\alpha$  expression levels following knockdown is clearly desirable in this type of study. Recently, distinct roles of  $\text{G}_q\alpha$  and  $\text{G}_{11}\alpha$  in mGlu1a receptor-mediated  $\text{Ca}^{2+}$  signaling in Purkinje neurons have been shown to result from differential expression levels of these two isoforms (Hartmann et al., 2004). Accordingly, it was shown that  $\text{G}_q\alpha$  was solely required for mGlu receptor-dependent synaptic transmission, whereas both  $\text{G}_q\alpha$  and  $\text{G}_{11}\alpha$  contributed to long-term depression in Purkinje neurons.

In the current study, we have used  $\text{G}_{q/11}\alpha$ -RNAi and  $\text{G}_q\alpha$  overexpression in combination with single cell  $\text{IP}_3$  and  $\text{Ca}^{2+}$  imaging as a novel approach to investigate the role of  $\text{G}_{q/11}\alpha$  expression in GPCR-mediated signaling. RNAi-knockdown of  $\text{G}_{q/11}\alpha$  protein expression was initially characterized in HEK cells stably expressing recombinant  $\text{M}_3$  mACh receptor. We then demonstrated the effects of RNAi and recombinant  $\text{G}_q\alpha$  expression on  $\text{IP}_3$  and  $\text{Ca}^{2+}$  signals generated by mGlu1 and mGlu5 receptors expressed recombinantly in CHO cells. By altering  $\text{G}_{q/11}\alpha$  expression levels, the agonist concentration-dependencies of these  $\text{G}_q$ PCRs were changed. Furthermore, the temporal profiles of  $\text{Ca}^{2+}$  signals generated indicate a central role for  $\text{G}_{q/11}\alpha$  in defining the nature of the response observed.

## Materials and Methods

**Cell Culture and Plasmid Transfection.** CHO cells stably expressing the human mGlu1a or mGlu5a receptor under the control of the inducible LacSwitch-II system (Stratagene) were maintained as described previously (Hermans et al., 1998; Nash et al., 2002) and are denoted as CHO-*lac*-mGlu1 or CHO-*lac*-mGlu5. HEK cells stably expressing the M<sub>3</sub> mACh receptor (HEK-m3) were created and maintained as described previously (Tovey and Willars, 2004). Plasmid containing the fusion construct between eGFP and the PH domain of PLC $\delta$ 1 (eGFP-PH<sub>PLC $\delta$</sub> ) was kindly donated by T. Meyer (Stanford University).

For single cell imaging experiments, CHO-*lac*-mGlu1/5 or HEK-m3 cells were grown on 25 mm coverslips and co-transfected 72 h prior to experimentation with 1.8  $\mu$ g G<sub>q/11</sub> $\alpha$ -RNAi, control RNAi, or full length human G<sub>q</sub> $\alpha$  and 0.2  $\mu$ g eGFP-PH<sub>PLC $\delta$</sub>  (for IP<sub>3</sub> imaging) or eGFP (for Ca<sup>2+</sup> imaging) using 6  $\mu$ l of GeneJuice (Novagen/EMD Biosciences) per coverslip. For induction of maximal mGlu receptor expression in CHO cells, the medium was replaced with fresh culture medium containing 100  $\mu$ M IPTG 18-20 h prior to experimentation. For standard SDS-PAGE immunoblotting, HEK-m3 cells were transfected in 6-well plates 72 h prior to experimentation with 2  $\mu$ g of G<sub>q/11</sub> $\alpha$ -RNAi or control RNAi using Lipofectamine2000. CHO cells were transfected in flasks (175 cm<sup>2</sup>) with 10  $\mu$ g of G<sub>q/11</sub> $\alpha$ -RNAi or control RNAi using 30  $\mu$ l GeneJuice and after 24 h, cells were seeded into 6-well plates for a further 48 h. For receptor biotinylation, real-time PCR and 6 M urea SDS-PAGE analysis, CHO cells were transfected using the Nucleofection system (Amaxa Biosystems), according to the manufacturer's optimized protocol. Briefly, 5x10<sup>6</sup> cells were transfected with 2  $\mu$ g of control- or G<sub>q/11</sub> $\alpha$ -RNAi and Program U-23 on the Nucleofector, before seeding cells into 6-well plates 72 h prior to experimentation.

**RNAi Design and Preparation.** To design an RNAi plasmid expressing G<sub>q/11</sub> $\alpha$ -specific small interfering RNA (siRNA), the mRNA sequences for human G<sub>q</sub> $\alpha$  (GenBank Accession NM\_002072) and G<sub>11</sub> $\alpha$  (GenBank Accession NM\_002067) were aligned to identify potential target sequences. Candidate 19 base pair sequences, homologous for both human G<sub>q</sub> $\alpha$  and G<sub>11</sub> $\alpha$  genes (and containing a G/C content of 40-60 %) were identified and gene specificity was checked using the BLASTN algorithm to search the GenBank sequence database. RNAi-expressing constructs for five selected sequences were created according to the manufacturer's instructions (using the *pSilencer*<sup>TM</sup> 1.0-U6 expression system, Ambion), and the knockdown of recombinantly expressed CFP-labeled G<sub>q</sub> $\alpha$  was used to assess the effectiveness of these constructs (data not shown). The target sequence selected for G<sub>q/11</sub> $\alpha$  silencing was 5'-GATGTTTCGTGGACCTGAAC-3', corresponding to positions 932-950,

relative to the start codon of human  $G_q$  and  $G_{11}$  (denoted as ' $G_{q/11}$ -RNAi'). Further, an additional control RNAi construct was generated (using the nucleotide sequence 5'-GCTGACCCTGGAGAGTTCATC-3'), and is denoted as 'control RNAi'.

**Immunoblot Analysis.** Levels of endogenous  $G_{q/11}\alpha$  protein expression in HEK-m3 and CHO-*lac*-mGlu1a cells were determined by a standard Western blot protocol (Willems and Kelly, 2001) using a  $G_{q/11}\alpha$ -specific antibody at 1:5000 dilution (CQ, kindly donated by G. Milligan, University of Glasgow). Antibodies against  $G_{i1-3}\alpha$  (1:2000; Santa Cruz),  $G_{12}\alpha$  (1:1000; Santa Cruz) and  $\gamma$ -tubulin (1:10,000; Sigma) were used as controls for RNAi specificity and protein loading. Antibodies against the C-terminal region of the mGlu1 receptor (1:1000; Chemicon International) and the C-terminal region of the mGlu5 receptor (1:1000; Upstate) respectively were used to detect mGlu1a and mGlu5a receptor expression. All primary antibody incubations were made at room temperature for 2 h or overnight at 4°C. Resolution of both  $G_q\alpha$  and  $G_{11}\alpha$  with an antibody (CQ) was achieved using SDS-PAGE gels containing 12.5% acrylamide and 6 M urea, as previously described (Milligan, 1993). The relative mobility of each  $G\alpha$  subunit was confirmed using cell lysates obtained from CHO-*lac*-mGlu cells recombinantly expressing human  $G_q\alpha$  or  $G_{11}\alpha$  using equivalent gels.

**Cell-Surface Biotinylation of mGlu1a and mGlu5a Receptors.** CHO-*lac*-mGlu1a and -mGlu5a cells were transiently transfected with  $G_{q/11}\alpha$ -RNAi, control RNAi or full length human  $G_q\alpha$  using the Amaxa Nucleofection system and seeded into 6 well plates. After 72 h, cells were washed twice with PBS at room temperature and labeled with membrane-impermeant EZ-Link™ Sulfo-NHS-biotin (1 mM in PBS) for 30 min at room temperature. Cells were washed twice with ice-cold PBS, once with 500 mM Tris/HCl (pH 7.4) and twice more with ice-cold PBS. Cells were then lysed for 10 min with solubilization buffer (10 mM Tris/HCl, 150 mM NaCl, 1 mM EDTA, 500  $\mu$ M EGTA, 1% Igepal, 0.1% SDS, pH 7.4) and centrifuged at 14,000  $xg$  for 5 min. The cleared supernatant (900  $\mu$ l) was then incubated with 200  $\mu$ l of streptavidin/agarose beads (diluted 1:10 in solubilization buffer) for 2 h with constant rotation at 4°C. The remaining supernatant was retained to assess receptor expression in whole cell lysates (see below). Beads were recovered by centrifugation during washed with 2 x 1 ml solubilization buffer and 2 x 1 ml PBS. Immunocomplexes were dissociated with 50  $\mu$ l of 2X sample buffer (125 mM Tris/HCl, 50 mM dithiothreitol (DTT), 4% sodium dodecylsulfate, 20% glycerol, 0.01% bromophenyl blue, pH 6.8), heated at 90°C for 5 min, and then resolved by SDS-PAGE (as described above). For total cell extracts, 20  $\mu$ l of the retained supernatant was diluted (1:1) with 2X sample buffer prior to SDS-PAGE.

**PCR Amplification of the RNAi Target Region from CHO Cells.** To determine the sequence of the RNAi target region of  $G_q\alpha$  and  $G_{11}\alpha$  derived from CHO cells, total RNA was isolated from CHO cells using the Qiagen RNeasy kit. Samples (200 ng RNA) were reverse transcribed into cDNA using the Omniscript RT-PCR kit (Qiagen). Primers specific for  $G_q\alpha$  and  $G_{11}\alpha$  based on rat sequence information (see Table 1) were used for PCR to amplify a 160 base pair fragment containing the RNAi target region using KOD HiFi DNA Polymerase (Novagen) as described in the manufacturer's instructions. PCR amplification was carried out over 30 cycles consisting of 98°C for 20 s, 50 or 52°C (for  $G_q\alpha$  and  $G_{11}\alpha$  primers, respectively) for 20 s and 72°C for 20 s. PCR reaction products were subsequently purified using a QIAquick PCR purification kit (Qiagen), and after gel electrophoresis the PCR product was extracted and purified using a QIAEX II Gel extraction kit (Qiagen). PCR products were sequenced directly using the same primers.

**Quantitative Real-Time PCR.** Following RNAi transfection, total RNA and cDNA were prepared from samples in triplicate, as described above. An RT negative control was included for each triplicate to control for genomic DNA contamination. Real-time PCR using SYBR-green fluorescence (Applied Biosystems) was carried out using an ABI 7700 machine as previously described (Medhurst et al., 2000). PCR parameters were 50°C for 2 min, 95°C for 10 min, 40 cycles of 95°C for 15 s and 60°C for 1 min. Real-time PCR data were captured using Sequence Detector Software (Applied Biosystems) to obtain  $C_t$  (threshold cycle) values for the gene of interest. Values were normalized against a housekeeping gene, cyclophilin, and expressed as % of control. All measurements were performed in triplicate for three separate transfections using the Amaxa Nucleofection system.

**Single Cell Imaging of  $IP_3$ .** Increases in cellular  $IP_3$  were detected by measuring the translocation of eGFP-PH<sub>PLC $\beta$</sub>  from the plasma membrane to the cytosol as described previously (Nash et al., 2002; Young et al., 2003). Cells were transfected as described above, and coverslips were mounted on the stage of an Olympus IX70 inverted epifluorescence microscope and perfused (5 ml min<sup>-1</sup>) at 37°C with Krebs-Henseleit buffer (KHB, in mM: NaCl 118, KCl 4.7, MgSO<sub>4</sub> 1.2, CaCl<sub>2</sub> 1.3, KH<sub>2</sub>PO<sub>4</sub> 1.2, NaHCO<sub>3</sub> 4.2, HEPES 10, glucose 11.7, pH 7.4) using a Gilson Minipuls 2 pump. Confocal images were collected after excitation at 488nm using an Olympus FV500 laser scanning confocal microscope at a scan rate of 1.5-2.5 Hz. eGFP-PH<sub>PLC $\beta$</sub>  translocation was measured by creating a region of interest in the cytosol and plotting the average pixel intensity in that region versus time. Data are expressed in relative fluorescent units (RFU) by subtraction of background fluorescence followed by dividing the fluorescent intensity at a given time by the initial fluorescence within each region of interest ( $F/F_0$ ). Drug applications were made using the perfusion line as indicated.



MOL Manuscript # 14258

**Ca<sup>2+</sup> Imaging.** Cells were transfected as described, and then loaded with fura-2AM (Molecular Probes) in 1 ml KHB (5  $\mu$ M final concentration) for 60-90 min. The cells were mounted on a Nikon Diaphot inverted epifluorescence microscope with an oil immersion objective (x40) and then excited at 340 and 380 nm (for fura-2AM) and 488 nm (for eGFP) using a Spectramaster II monochromator (PerkinElmer Life Sciences) at a sample rate of 0.7 Hz. GFP-containing cells were identified (as a marker of G<sub>q/11</sub> $\alpha$ -RNAi/control RNAi/G<sub>q</sub> $\alpha$  transfected cells) and sequential images were then captured from GFP-transfected cells at wavelengths above 510 nm following drug applications made using the perfusion line as indicated. Ca<sup>2+</sup> signals are expressed as 340:380 nm ratios.

**Data Analysis.** Curve fitting of data and calculation of EC<sub>50</sub> values was carried out using Prism 3.0 Software (GraphPad Software, Inc., San Diego, CA). Statistical differences between datasets were determined by one-way analysis of variance (ANOVA) for multiple comparisons, followed by Bonferroni's multiple-range test at  $p < 0.05$  (using Prism 3.0 software), or Student's *t*-test (unpaired;  $p < 0.05$  being considered significant).

## Results

**RNAi-Mediated Knockdown of  $G_{q/11}\alpha$  Protein Expression and Function in HEK Cells Stably Expressing the  $M_3$  mACh Receptor.** RNAi constructs designed using 19 base pair sequences targeting homologous regions of human  $G_q\alpha$  and  $G_{11}\alpha$  protein expression were initially tested in HEK-m3 cells. Immunoblotting experiments revealed robust silencing of  $G_{q/11}\alpha$  72 h after transfection with  $G_{q/11}\alpha$ -RNAi compared to control RNAi. In these experiments, the transfection efficiency typically achieved was ~50%, suggesting a high degree of  $G_{q/11}\alpha$  silencing in individual HEK cells. Antibodies detecting  $\gamma$ -tubulin and G protein  $\alpha$ -subunits,  $G_{i1-3}\alpha$ , confirmed equal protein loading (Fig. 1A).

Single-cell  $IP_3$  imaging, using cells transfected with eGFP-PH<sub>PLC $\delta$</sub>  alone, showed a concentration-dependent increase in cytosolic fluorescence in response to 30 s applications of methacholine, with a best-fit  $EC_{50}$  of 0.9  $\mu$ M. This was unaffected by co-transfection with control RNAi, but was inhibited by  $G_{q/11}\alpha$ -RNAi, as demonstrated by a rightward shift in the concentration-response curve ( $EC_{50}$  6  $\mu$ M) and a suppressed maximal response (2-fold, compared to 3.5-fold over basal in control cells, shown in Fig. 1B). Representative images (Fig. 1B) showed a clear suppression of eGFP-PH<sub>PLC $\delta$</sub>  translocation from the plasma membrane to the cytosol in  $G_{q/11}\alpha$ -RNAi containing cells compared to control RNAi, and also indicate that these cells display no obvious morphological changes.

**RNAi-Mediated Knockdown of  $G_{q/11}\alpha$  Protein Expression in CHO Cells.** Having identified a functional  $G_{q/11}\alpha$ -RNAi construct in HEK cells, we tested the same construct in CHO cell lines stably and inducibly expressing mGlu1 and mGlu5 receptors. Immunoblotting showed a significant inhibition of endogenous  $G_{q/11}\alpha$  expression 72 h post-transfection with  $G_{q/11}\alpha$ -RNAi, compared to control RNAi cells (Fig. 2A). The transfection efficiency typically achieved in CHO cells was 40-50% (determined using GFP, data not shown) again suggesting highly efficient  $G_{q/11}\alpha$  protein silencing. Importantly,  $G_{i1-3}\alpha$ ,  $G_{12}\alpha$  and  $\gamma$ -tubulin protein expression levels were unaffected (Fig. 2A). Further experiments confirmed that induction of mGlu1 and mGlu5 receptor expression was unaffected by RNAi treatment (Fig. 2B).

Following the identification of an RNAi construct with  $G_{q/11}\alpha$  silencing activity in both human and CHO cell backgrounds, the 19 base pair RNAi target sequence within  $G_q\alpha$  and  $G_{11}\alpha$  derived from the CHO cell line was investigated. No sequence information for Chinese hamster  $G_{q/11}\alpha$  was available in the GenBank/EMBL databases. We therefore amplified the

appropriate regions from CHO cells by PCR with  $G_q\alpha$ - and  $G_{11}\alpha$ -selective primers, based on rat sequence information (see Table 1). Sequencing of the amplicons from CHO cells indicated two base pair differences (corresponding to C→T changes at positions 9 and 21 in Fig. 3A) in  $G_{11}\alpha$  compared to CHO  $G_q\alpha$  and human  $G_{q/11}\alpha$ .

In view of the contrasting reports of RNAi specificity in the literature, it was imperative to assess the knockdown of  $G_q\alpha$  relative to  $G_{11}\alpha$ . Using the Nucleofection system to achieve optimal plasmid transfection (>80% determined using GFP, data not shown) and real-time PCR with  $G_q\alpha$ - and  $G_{11}\alpha$ -specific primers (Table 1), a robust knockdown (approx. 75%) of  $G_q\alpha$  mRNA in both mGlu1 and mGlu5 receptor-expressing CHO-*lac* cells was observed (Fig. 3B). Unexpectedly,  $G_{11}\alpha$  knockdown was also observed in the same experiments.  $G_q\alpha$  and  $G_{11}\alpha$  knockdown was normalized to cyclophilin mRNA levels, which were unaffected following  $G_{q/11}\alpha$ -RNAi transfection. To complement the mRNA analysis, SDS-PAGE gels containing 6 M urea were used to resolve  $G_q\alpha$  and  $G_{11}\alpha$  proteins in these cells (see Materials and Methods). Under these conditions  $G_{11}\alpha$  migrates further than  $G_q\alpha$ , an observation confirmed using lysates obtained from CHO-*lac*-mGlu cells recombinantly expressing human  $G_q\alpha$  and  $G_{11}\alpha$  in equivalent gels (Fig. 3C). Assuming that the antibody-immunoreactivity for both  $G\alpha$  subunits is comparable, these data suggest that expression levels of  $G_q\alpha$  and  $G_{11}\alpha$  proteins under control conditions in CHO-*lac*-mGlu1a cells are similar. The relative reduction of  $G_q\alpha$  and  $G_{11}\alpha$  protein expression was similar to the reduction in  $G_q\alpha$  and  $G_{11}\alpha$  mRNA levels determined by real-time PCR. A reduction of  $G_q\alpha$  mRNA by approx. 75% corresponded to an almost complete knockout of  $G_q\alpha$  protein, and similarly a reduction in  $G_{11}\alpha$  mRNA by approx. 60% led to a slightly less efficient knockdown of  $G_{11}\alpha$  protein expression. The relationship between mRNA and protein knockdown is dependent on the turnover of  $G_q\alpha$  and  $G_{11}\alpha$  proteins. A previous study in CHO cells reported that the half-time of  $G_{q/11}\alpha$  is 18 h (Mitchell et al., 1993). Levels of  $G_{i1-3}\alpha$ ,  $G_{12}\alpha$  and  $\gamma$ -tubulin protein expression in these experiments were unaffected (data not shown). These experiments demonstrate the effectiveness of RNAi in silencing both  $G_q\alpha$  and  $G_{11}\alpha$ , and so provide evidence that mismatches in the RNAi target sequence are tolerated, at least for these closely related gene products.

**Effects of Manipulating  $G_{q/11}\alpha$  Expression on Cell-Surface Receptor Expression.** To examine the possibility that up- or down-regulation of  $G_{q/11}\alpha$  protein expression can influence mGlu1/5 receptor trafficking to the plasma membrane, we utilized a cell-surface protein biotinylation strategy. In both CHO-*lac*-mGlu1a (Fig. 4A) and mGlu5a (Fig. 4B) cells,  $G_{q/11}\alpha$  protein expression was increased or decreased by transient transfection with human

recombinant  $G_q\alpha$  or  $G_{q/11}\alpha$ -RNAi, respectively. For mGlu1a and mGlu5a receptors, doublet immunoreactive bands were evident at approx. 150 KDa. mGlu1a and mGlu5a receptor cell-surface biotinylation indicated that the mature, higher molecular weight protein (upper band) is enriched at the plasma membrane (Fig. 4A and B). Importantly, altering  $G_{q/11}\alpha$  expression levels did not affect cell-surface mGlu1a and mGlu5a receptor, or indeed total receptor expression in whole cell extracts, indicating that the trafficking/localization of these receptors to the plasma membrane is independent of  $G_{q/11}\alpha$  protein expression.

### **The Effects of Manipulating $G_{q/11}\alpha$ Protein Expression on Single Cell $IP_3$ Levels.**

Measurements of  $IP_3$  production in cells transfected with  $G_{q/11}\alpha$ -RNAi, control RNAi or full-length human  $G_q\alpha$  were made possible by co-transfection of the  $IP_3$  biosensor, eGFP-PH<sub>PLC $\delta$</sub> . In all of the control RNAi CHO-*lac*-mGlu1a cells examined, a graded increase in eGFP-PH<sub>PLC $\delta$</sub>  translocation was observed in response to incremental glutamate concentrations, each applied for 30 s (Fig. 5), with a best-fit EC<sub>50</sub> of 8.4  $\mu$ M for the peak  $IP_3$  response. In CHO-*lac*-mGlu1a cells transfected with  $G_{q/11}\alpha$ -RNAi, responses to glutamate were almost abolished, with no translocation of eGFP-PH<sub>PLC $\delta$</sub>  observed in several individual cells. In contrast, when cells were transfected with full-length human  $G_q\alpha$ , the EC<sub>50</sub> for the peak  $IP_3$  response left-shifted from 8.4  $\mu$ M to 2.0  $\mu$ M glutamate ( $p < 0.05$ ), while the maximal responsiveness was not significantly affected ( $p > 0.05$ ; Fig. 5).

Single cell mGlu5a receptor-induced  $IP_3$  responses underlying oscillatory  $Ca^{2+}$  signals have been studied extensively in CHO-*lac*-mGlu5a cells (Nash et al., 2002; Nahorski et al., 2003; Young et al., 2003). To examine the effect of manipulating  $G_{q/11}\alpha$ -protein levels, cells were transfected with  $G_{q/11}\alpha$ -RNAi, control RNAi or full-length human  $G_q\alpha$ . Responses to a single maximal concentration (30  $\mu$ M) of glutamate were subsequently examined over a 300 s time period for each treatment. Within a population of control cells, mGlu5a receptor-induced  $IP_3$  increases in response to glutamate eGFP-PH<sub>PLC $\delta$</sub>  translocation were not detected in 38% of cells (denoted as non-responders in Fig. 6A and 6B). In control RNAi cells where eGFP-PH<sub>PLC $\delta$</sub>  translocation was measurable, the predominant response was a peak elevation of  $IP_3$  followed by repetitive oscillations until agonist washout (denoted as oscillatory in Fig. 6A and 6B). In several cells (24% of the total number of cells), no detectable change in  $IP_3$  was detected following the initial peak increase (denoted as single spike in Fig. 6A). In CHO-*lac*-mGlu5a cells transfected with  $G_{q/11}\alpha$ -RNAi, repetitive oscillations in  $IP_3$  were still observed. However, the number of non-responders and single spike responses increased to 86% (from 62%) of the total number of cells. In contrast, following full-length  $G_q\alpha$  transfection, the

number of non-responding cells decreased to 25% of the total population and only a relatively low number of cells (8%) exhibited IP<sub>3</sub> oscillations. Instead, in 50% of G<sub>q</sub>α-transfected cells, IP<sub>3</sub> signals were manifested as an initial peak followed by a sustained plateau response until agonist washout (denoted as saturating in Fig. 6A and 6B). In addition, the mean increase in peak IP<sub>3</sub> production was at least two-fold higher in G<sub>q</sub>α-transfected cells (0.37 ± 0.07 RFU; *p*<0.05), compared to control (0.17 ± 0.03 RFU) and RNAi-transfected cells (0.13 ± 0.05 RFU) (Fig. 6C).

**G<sub>q/11</sub>α Protein Expression Levels Influence Stimulus-Strength and the Temporal Profile of mGlu Receptor-Mediated Ca<sup>2+</sup> Mobilization.** Previous studies from our laboratory have made real-time concurrent measurements of mGlu1a receptor generated IP<sub>3</sub> and Ca<sup>2+</sup><sub>i</sub> in single cells (Nash et al., 2001). During prolonged activation, these receptors give an initial transient peak in IP<sub>3</sub> production followed by a sustained plateau phase which is closely mirrored by a peak and sustained plateau Ca<sup>2+</sup> response. In contrast, the mGlu5a receptor produces oscillatory IP<sub>3</sub> and Ca<sup>2+</sup> signals (Nash et al., 2001, 2002; Nahorski et al., 2003). In the current study, the effects of manipulating G<sub>q/11</sub>α protein levels on the glutamate concentration-dependency and temporal profile of mGlu1a and mGlu5a receptor-mediated Ca<sup>2+</sup> signaling were investigated. Receptors were therefore exposed to incremental increases in glutamate (1 to 100 μM, 200 s at each concentration) to determine the role of G<sub>q/11</sub>α expression levels on complex calcium signals.

In control RNAi and G<sub>q</sub>α-expressing CHO-*lac*-mGlu1a cells, ~60% of transfected cells responded to glutamate with an initial peak elevation in Ca<sup>2+</sup> followed by a sustained plateau phase. Following G<sub>q/11</sub>α-RNAi transfection however, 84% (66 out of 79) of cells elicited transient peak increases in Ca<sup>2+</sup> mobilization without a sustained phase even at maximal concentrations of glutamate (Fig. 7C, denoted as ‘non-saturating’). These non-saturating responses most often occurred as a single base-line spike coincident with agonist addition (as illustrated with the representative trace in Fig. 7A). However, on occasion additional intermittent spikes were evident, perhaps signifying oscillations occurring as a result of regenerative CICR. The few cells that did actually initiate a sustained peak and plateau did so only at high concentrations of agonist (7 out of 66 cells over four experiments). Changing levels of G<sub>q/11</sub>α-protein expression altered the glutamate concentration threshold for the onset of mGlu1a receptor-induced Ca<sup>2+</sup> responses (Fig. 8A). Thus, in control RNAi cells, the initial onset of Ca<sup>2+</sup> mobilization occurred at either 3 or 10 μM glutamate (35 and 50% of the total number of cells, respectively), which correlates with the IP<sub>3</sub> measurements made in these cells

(Fig. 5). In  $G_{q/11}\alpha$ -RNAi transfected cells a greater agonist concentration was required to produce significant increases in  $IP_3$  (around 10  $\mu$ M glutamate) reflecting a shift to higher agonist concentrations for the onset of  $Ca^{2+}$  mobilization (only 14% responded to 3  $\mu$ M, with 53% responding to 10  $\mu$ M). Furthermore, 25% of  $G_{q/11}\alpha$ -RNAi-transfected cells compared to 8% of control cells only responded to concentrations greater than 10  $\mu$ M glutamate. The shift in stimulus threshold was further exemplified in experiments using  $G_q\alpha$  over-expression, where 3  $\mu$ M glutamate mediated a large increase in  $IP_3$  (Fig. 5), so that 74% (25 out of 34) of cells at this concentration of glutamate were able to initiate a  $Ca^{2+}$  signal compared to 35% of control cells (Figs. 7 and 8A). Clearly in the mGlu1a model system,  $G_{q/11}\alpha$  expression levels regulate the efficacy and the nature of agonist-mediated receptor activation. This is manifested as altered levels of  $IP_3$  production and hence differential  $Ca^{2+}$  signals in response to increasing agonist concentrations. In contrast, mGlu5a receptor signaling is relatively independent of stimulus-strength over a wide agonist concentration range (Nash et al., 2002), and it was not clear what effect alterations in  $G_{q/11}\alpha$  protein levels would have.

In control RNAi mGlu5a receptor-expressing cells, increasing concentrations of glutamate produced non-saturating  $Ca^{2+}$  oscillations (Fig. 7B and 7D). Although in many cells the frequency of  $Ca^{2+}$  oscillations was initially sensitive to the increase in agonist concentration, in all cases the  $Ca^{2+}$  frequency quickly became insensitive to agonist concentration, which is indicative of oscillations driven by PKC-dependent feedback on the receptor (see Nash et al., 2002; Fig. 7B, representative trace). Similar observations were made from mGlu5a receptor-expressing cells transfected with  $G_{q/11}\alpha$ -RNAi, but in the majority of cells the onset of response occurred at higher concentrations of agonist (Fig. 8B; 10  $\mu$ M versus 3  $\mu$ M glutamate in control cells), and consequently non-saturating  $Ca^{2+}$  oscillations in most  $G_{q/11}\alpha$ -RNAi transfected cells could not be identified until concentrations of  $\geq 10$   $\mu$ M were used (Fig. 7, representative trace). In CHO-*lac*-mGlu5a cells transfected with  $G_q\alpha$  75% (52 out of 69 cells) cells responded at 1  $\mu$ M glutamate. A key effect of  $G_q\alpha$  over-expression was the observation of mGlu5 cells exhibiting saturating  $Ca^{2+}$  responses to increasing concentrations of glutamate (Fig 7B and 7D). Thus, although oscillatory responses were observed at low glutamate concentrations, these rapidly converted to a sustained plateau response upon increases in agonist concentrations. In this way the  $Ca^{2+}$  response mirrored the  $IP_3$  signals produced by the mGlu5a receptor in recombinant  $G_q\alpha$ -expressing cells (Fig. 6B).

## Discussion

Complex  $G_{q/11}$ -coupled receptor-mediated  $Ca^{2+}$  signals enable a wide range of cellular processes to be regulated (Berridge et al., 2000). Classically, low levels of receptor occupancy are known to induce small steady-state increases in  $IP_3$  that evoke oscillatory  $Ca^{2+}$  signals, the frequency of which is sensitive to agonist concentration. Higher levels of  $IP_3$  generation caused by more intense receptor stimulation can lead to larger, peak-and-plateau type  $Ca^{2+}$  responses. Studies using the  $IP_3$  biosensor, eGFP-PH<sub>PLC $\delta$</sub> , have since shown that  $Ca^{2+}$  oscillations can also occur in synchrony with  $IP_3$  oscillations, as described in ATP-stimulated canine kidney epithelial cells (Hirose et al., 1999) or stimulation of mGlu5 receptors in CHO cells (Nash et al., 2001). Oscillations in  $IP_3$  are likely to occur as a result of negative feedback regulation by PKC (Codazzi et al., 2001; Nash et al., 2002; Young et al., 2002) or RGS proteins (Luo et al., 2001), but also by a positive feedback effect of  $Ca^{2+}$  to enhance PLC activity (Young et al., 2003). For the mGlu5a receptor, synchronous  $IP_3$  and  $Ca^{2+}$  oscillations occur via a PKC-dependent dynamic uncoupling of the receptor from its G protein by phosphorylation of a specific residue on the receptor (Kawabata et al., 1996; Kim et al., 2005). As the substrate for PKC is the receptor, this provides a mechanism by which the frequency of  $Ca^{2+}$  oscillations are regulated by receptor density in addition to agonist concentration, as shown for the mGlu5 receptor (Nash et al., 2002). The mGlu1 receptor lacks this critical consensus sequence and is not subject to this feedback regulation. Therefore, mGlu1 receptor activation can initiate sustained, peak-and-plateau  $Ca^{2+}$  responses. These studies suggest that  $Ca^{2+}$  signals initiated by  $G_{q/11}$ -coupled GPCRs are susceptible to regulation by a number of factors, including receptor-G protein coupling efficiency, receptor density, agonist concentration and sensitivity to feedback mechanisms.

The fine-tuning of  $Ca^{2+}$  signals by these factors may account for contrasting patterns of mGlu5 receptor-driven  $Ca^{2+}$  oscillations in different cell backgrounds (Codazzi et al., 2001; Dale et al., 2001; Nash et al., 2002). In the current study we have extended these investigations by assessing the contribution of  $G_{q/11}\alpha$  protein expression levels in generating distinct  $IP_3$  and  $Ca^{2+}$  signaling patterns mediated by group I mGlu receptors. Using RNAi or recombinant  $G_q\alpha$  expression in combination with an  $IP_3$  biosensor or  $Ca^{2+}$  sensitive dye, we have been able to study the concentration-dependency and the temporal profile of  $IP_3$  and  $Ca^{2+}_i$  in single cells in real-time.

The use of RNAi as an approach to gene silencing has now been extensive although its mechanism is not yet fully understood (Dykxhoorn et al., 2003; Hannon and Rossi, 2004; Meister and Tuschl, 2004). The enormous interest in this technique has also highlighted potential limitations, in particular with respect to RNAi specificity (Hannon and Rossi, 2004; Snove and Holen, 2004). Here, we have shown a robust RNAi-induced silencing of  $G_{q/11}\alpha$  protein expression in HEK-m3 cells, which resulted in a suppression of the methacholine-induced  $IP_3$  signal. Very recently, effective silencing of  $G_{q/11}\alpha$  proteins in HEK cells has been reported in two other studies, using an identical RNAi sequence to the one used here. Using an siRNA approach, the authors established a role for  $G_{q/11}\alpha$  proteins in stress fiber formation (Barnes et al., 2005), but not chemotaxis (Hunton et al., 2005), following angiotensin II  $AT_{1A}$  receptor activation.

Effective  $G_{q/11}\alpha$  silencing was also observed in CHO-*lac* cell lines stably expressing mGlu1 or mGlu5 receptors, with no effect on the expression levels of  $G_{i1-3}\alpha$  and  $G_{12}\beta$  proteins or the receptors themselves. Despite the presence of a two base-pair mismatch in the RNAi target region of  $G_{11}\alpha$  compared to  $G_q\alpha$  in the Chinese hamster cell model, real-time PCR and a pan- $G_{q/11}\alpha$  antibody revealed knockdown of both  $G_q\alpha$  and  $G_{11}\alpha$ . Several reports have described similar tolerance of mismatches between siRNA and target mRNA, especially when these occur at the periphery of the target sequence (Amarzguioui et al., 2003; Vickers et al., 2003; Snove and Holen, 2004). Other studies also indicate that siRNAs containing mismatches can act as endogenous microRNAs to inhibit translation, but not to cause significant mRNA degradation (Doench et al., 2003; Saxena et al., 2003). However, this was not the case here, as we observed a clear reduction in mRNA and protein expression. The effect therefore appears to be specific to  $G_q\alpha$  and  $G_{11}\alpha$  as a result of the close homology of the two sequences in the target region, instead of generic knockdown of unrelated proteins. In this study we have therefore been able to use the RNAi construct to assess the effects of combined  $G_{q/11}\alpha$  knockdown, but in doing so also provide evidence for a 'cross-reactivity' of siRNA targeting closely related genes.

Knockdown of  $G_{q/11}\alpha$  protein almost completely eliminated mGlu1a receptor-mediated  $IP_3$  responses in single cells at maximal concentrations of agonist, whereas increased  $G_q\alpha$  expression produced a significant enhancement in agonist sensitivity. Despite the ability of mGlu1a receptors to couple to other G proteins, such as  $G_i\alpha$ , which can contribute to phosphoinositide turnover (Hermans and Challiss, 2001), our current data suggest that  $G_{q/11}\alpha$  coupling alone accounts for the majority of PLC activation in this expression system. Reducing



the expression level of  $G_{q/11}\alpha$  clearly affected the signaling properties of mGlu1a receptor, so that the subsequent  $Ca^{2+}$  response no longer resembled the characteristic sustained peak-and-plateau signal typical of this receptor subtype (Kawabata et al., 1996; Nash et al., 2001). Instead, the observed baseline  $Ca^{2+}$  spiking was likely to be the result of regenerative CICR associated with small increments in  $IP_3$  (Bootman et al., 1996; Thomas et al., 1996; Nash et al., 2001; Young et al., 2003). This finding supports the notion that the temporal response initiated by the mGlu1a receptor is stimulus-strength-dependent and is likely to be influenced by receptor *and* G protein expression levels.

$Ca^{2+}$  signals activated by the mGlu5 receptor were also sensitive to changes in  $G_{q/11}\alpha$  expression. Using recombinant  $G_q\alpha$  expression we have revealed an ability of mGlu5 receptor to overcome PKC-dependent feedback allowing the receptor to mediate plateau  $IP_3$  and  $Ca^{2+}$  responses. In cells transfected with recombinant  $G_q\alpha$ , peak  $IP_3$  responses were clearly enhanced, and  $Ca^{2+}$  mobilization was achieved at lower threshold concentrations of agonist. This supports our previous proposal (Nash et al., 2002) and suggests that increased PLC activation reduces the period of PKC-dependent uncoupling and favors transition to sustained  $Ca^{2+}$  mobilization. With increased coupling and PLC activation the mGlu5 receptor therefore mirrors  $M_3$  mACh receptor signaling in lacrimal acinar cells, where PKC feedback occurs over a defined agonist concentration range (Bird et al., 1993). It is likely that sustained activation occurs when  $IP_3$  receptors are saturated leading to store depletion and capacitative  $Ca^{2+}$  entry. Indeed, previous studies have demonstrated mGlu5 receptor-activated peak-and-plateau responses in the CHO-*lac*-mGlu5a cell-model following thapsigargin-induced depletion of intracellular  $Ca^{2+}$  stores (Nash et al., 2002). Using RNAi, we have shown that a reduction in mGlu5 receptor stimulus-strength restricts  $IP_3$  production, even at maximal concentrations of agonist, and constrains  $Ca^{2+}$  responses to baseline oscillations that require higher concentrations of agonist for initiation. Although PKC dependency was not tested here, previous studies in the same cells have shown that PKC down-regulation can prevent  $IP_3$  oscillations, such that maximal concentrations of agonist initiate sustained peak-and-plateau  $Ca^{2+}$  responses in a similar manner to the mGlu1a receptor (Nash et al., 2002). Importantly, at lower concentrations of agonist PKC-independent  $Ca^{2+}$  oscillations were seen, which were sensitive to agonist concentration and may reflect the  $Ca^{2+}$  oscillations observed in some cells following RNAi treatment in the present experiments.

In conclusion, we have shown that altering  $G_{q/11}\alpha$  expression markedly alters the temporal profile and agonist concentration-dependencies of  $IP_3$  and  $Ca^{2+}$  signals generated

following either mGlu1a or mGlu5a receptor activation. This work also demonstrates that regulating  $G_{q/11}\alpha$  expression levels can fundamentally alter the signaling properties of the mGlu5 receptor subtype. For the mGlu5 receptor it appears that the predominant dynamic uncoupling mechanism linking receptor activation to  $Ca^{2+}$  signaling instills particular emergent properties. Thus, while the receptor expression level primarily determines the  $Ca^{2+}$  oscillatory frequency, the transitions between CICR, dynamic uncoupling and peak-and-plateau behaviors are modulated by the level of  $G_{q/11}$  expression. It will be interesting to establish the effects of changing the levels of other intermediates in the signaling pathway (e.g. PLC $\beta$  expression), or the presence of Homer proteins (Fagni et al., 2000; Kiselyov et al., 2003) on mGlu1/5 receptor signaling. It is also interesting to speculate on whether translocation of mGlu5 receptors to the plasma membrane from an intracellular locus (Hubert et al., 2001), and/or direct or indirect (e.g. through changes in RGS protein expression) changes in G protein expression/function, can fundamentally alter neuronal  $Ca^{2+}$  signaling by this receptor subtype under altered physiological or pathophysiological conditions.

### **Acknowledgements**

The authors wish to thank Drs. Melanie Robbins, Isabel Benzel and Andrew Calver (GlaxoSmithKline, Harlow, UK) for their expert technical guidance on RT-PCR and helpful discussion. We also thank Dr. Mark Nash (Novartis Institute of Medical Sciences, London) for his initial input and ongoing intellectual contribution to this research project.

## References

- Amarzguioui M, Holen T, Babaie E, and Prydz H (2003) Tolerance for mutations and chemical modifications in a siRNA. *Nucleic Acids Res* **31**:589-595.
- Barnes WG, Reiter E, Violin JD, Ren X-R, Milligan G, and Lefkowitz RJ (2005)  $\beta$ -Arrestin 1 and  $G\alpha_{q/11}$  coordinately activate RhoA and stress fiber formation following receptor stimulation. *J Biol Chem* **280**:8041-8050.
- Berridge MJ, Lipp P, and Bootman MD (2000) The versatility and universality of calcium signalling. *Nat Rev Mol Cell Biol* **1**:11-21.
- Bird GS, Rossier MF, Obie JF, and Putney JW (1993) Sinusoidal oscillations in intracellular calcium requiring negative feedback by protein kinase C. *J Biol Chem* **268**:8425-8428.
- Bootman MD, Young KW, Young JM, Moreton RB, and Berridge MJ (1996) Extracellular calcium concentration controls the frequency of intracellular calcium spiking independently of inositol 1,4,5-trisphosphate production in HeLa cells. *Biochem J* **314**:347-354.
- Codazzi F, Teruel MN, and Meyer T (2001) Control of astrocyte  $Ca^{2+}$  oscillations and waves by oscillating translocation and activation of protein kinase C. *Curr Biol* **11**:1089-1097.
- Dale LB, Babwah AV, Bhattacharya M, Kelvin DJ, and Ferguson SSG (2001) Spatial-temporal patterning of metabotropic glutamate receptor-mediated inositol 1,4,5-trisphosphate, calcium, and protein kinase C oscillations - Protein kinase C-dependent receptor phosphorylation is not required. *J Biol Chem* **276**:35900-35908.
- Davignon I, Catalina MD, Smith D, Montgomery J, Swantek J, Croy J, Siegelman M, and Wilkie TM (2000) Normal hematopoiesis and inflammatory responses despite discrete signaling defects in  $G\alpha_{15}$  knockout mice. *Mol Cell Biol* **20**:797-804.
- Doench JG, Petersen CP, and Sharp PA (2003) siRNAs can function as miRNAs. *Genes Dev* **17**:438-442.
- Dykxhoorn DM, Novina CD, and Sharp PA (2003) Killing the messenger: short RNAs that silence gene expression. *Nat Rev Mol Cell Biol* **4**:457-467.
- Fagni L, Chavis P, Ango F, and Bockaert J (2000) Complex interactions between mGluRs, intracellular  $Ca^{2+}$  stores and ion channels in neurons. *Trends Neurosci* **23**:80-88.
- Greif GJ, Sodickson DL, Bean BP, Neer EJ, and Mende U (2000) Altered regulation of potassium and calcium channels by GABA<sub>B</sub> and adenosine receptors in hippocampal neurons from mice lacking  $G\alpha_o$ . *J Neurophysiol* **83**:1010-1018.
- Haley JE, Abogadie FC, Delmas P, Dayrell M, Vallis Y, Milligan G, Caulfield MP, Brown DA, and Buckley NJ (1998) The  $\alpha$ -subunit of  $G_q$  contributes to muscarinic inhibition of the M-type potassium current in sympathetic neurons. *J Neurosci* **18**:4521-4531.
- Hannon GJ, and Rossi JJ (2004) Unlocking the potential of the human genome with RNA interference. *Nature* **431**:371-378.
- Hartmann J, Blum R, Kovalchuk Y, Adelsberger H, Kuner R, Durand GM, Miyata M, Kano M, Offermanns S, and Konnerth A (2004) Distinct roles of  $G\alpha_q$  and  $G\alpha_{11}$  for Purkinje cell signaling and motor behavior. *J Neurosci* **24**:5119-130.
- Hermans E, and Challiss RA (2001) Structural, signalling and regulatory properties of the group I metabotropic glutamate receptors: prototypic family C G-protein-coupled receptors. *Biochem J* **359**:465-484.
- Hermans E, Young KW, Challiss RAJ, and Nahorski SR (1998) Effects of human type 1a metabotropic glutamate receptor expression level on phosphoinositide and  $Ca^{2+}$  signalling in an inducible cell expression system. *J Neurochem* **70**:1772-1775.
- Hirose K, Kadowaki S, Tanabe M, Takeshima H, and Iino M (1999) Spatiotemporal dynamics of inositol 1,4,5-trisphosphate that underlies complex  $Ca^{2+}$  mobilization patterns. *Science* **284**:1527-1530.
- Hubert GW, Paquet M, and Smith Y (2001) Differential subcellular localization of mGluR1a and mGluR5a in the rat and monkey Substantia nigra. *J Neurosci* **21**:1838-1847.
- Hunton DL, Barnes WG, Kim J, Ren X-R, Violin JD, Reiter E, Milligan G, Patel DD, and Lefkowitz RJ (2005)  $\beta$ -Arrestin 2-dependent angiotensin II type 1A receptor-mediated pathway of chemotaxis. *Mol Pharmacol* **67**:1229-1236.

- Kawabata S, Tsutsumi R, Kohara A, Yamaguchi T, Nakanishi S, and Okada M (1996) Control of calcium oscillations by phosphorylation of metabotropic glutamate receptors. *Nature* **383**:89-92.
- Kim CH, Braud S, Isaac JT, and Roche KW (2005) Protein kinase C phosphorylation of the metabotropic glutamate receptor mGluR5 on serine-839 regulates Ca<sup>2+</sup> oscillations. *J Biol Chem* **280**:25409-25415.
- Kiselyov K, Shin DM, and Muallem S (2003) Signalling specificity in GPCR-dependent Ca<sup>2+</sup> signalling. *Cell Signal* **15**:243-253.
- Luo X, Popov S, Bera AK, Wilkie TM, and Muallem S (2001) RGS proteins provide biochemical control of agonist-evoked [Ca<sup>2+</sup>]<sub>i</sub> oscillations. *Mol Cell* **7**:651-660.
- Macrez-Lepretre N, Kalkbrenner F, Schultz G, and Mironneau J (1997) Distinct functions of G<sub>q</sub> and G<sub>11</sub> proteins in coupling  $\alpha_1$ -adrenoreceptors to Ca<sup>2+</sup> release and Ca<sup>2+</sup> entry in rat portal vein myocytes. *J Biol Chem* **272**:5261-5268.
- Medhurst AD, Harrison DC, Read SJ, Campbell CA, Robbins MJ, and Pangalos MN (2000) The use of TaqMan RT-PCR assays for semi-quantitative analysis of gene expression in CNS tissues and disease models. *J Neurosci Methods* **98**:9-20.
- Meister G, and Tuschl T (2004) Mechanisms of gene silencing by double-stranded RNA. *Nature* **431**:343-349.
- Milligan G (1993) Regional distribution and quantitative measurement of the phosphoinositidase C-linked guanine nucleotide binding proteins G<sub>11</sub> $\alpha$  and G<sub>q</sub> $\alpha$  in rat brain. *J Neurochem* **61**:845-851.
- Mitchell FM, Buckley NJ, and Milligan G (1993) Enhanced degradation of the phosphoinositidase C-linked guanine-nucleotide-binding protein G<sub>q</sub> $\alpha$ /G<sub>11</sub> $\alpha$  following activation of the human M<sub>1</sub> muscarinic acetylcholine receptor expressed in CHO cells. *Biochem J* **293**:495-499.
- Nahorski SR, Young KW, Challiss RAJ, and Nash MS (2003) Visualizing phosphoinositide signalling in single neurons gets a green light. *Trends Neurosci* **26**:444-452.
- Nash MS, Schell MJ, Atkinson PJ, Johnston NR, Nahorski SR, and Challiss RAJ (2002) Determinants of metabotropic glutamate receptor-5-mediated Ca<sup>2+</sup> and inositol 1,4,5-trisphosphate oscillation frequency. Receptor density versus agonist concentration. *J Biol Chem* **277**:35947-35960.
- Nash MS, Young KW, Challiss RAJ, and Nahorski SR (2001) Intracellular signalling. Receptor-specific messenger oscillations. *Nature* **413**:381-382.
- Offermanns S (2003) G-proteins as transducers in transmembrane signalling. *Prog Biophys Mol Biol* **83**:101-130.
- Saxena S, Jonsson ZO, and Dutta A (2003) Small RNAs with imperfect match to endogenous mRNA repress translation. Implications for off-target activity of small inhibitory RNA in mammalian cells. *J Biol Chem* **278**:44312-44319.
- Snoe O, and Holen T (2004) Many commonly used siRNAs risk off-target activity. *Biochem Biophys Res Commun* **319**:256-263.
- Taylor CW, and Thorn P (2001) Calcium signalling: IP<sub>3</sub> rises again...and again. *Curr Biol* **11**:R352-R355.
- Thomas AP, Bird GS, Hajnoczky G, Robb-Gaspers LD, and Putney JW (1996) Spatial and temporal aspects of cellular calcium signaling. *FASEB J* **10**:1505-1517.
- Tovey SC, and Willars GB (2004) Single-cell imaging of intracellular Ca<sup>2+</sup> and phospholipase C activity reveals that RGS 2, 3, and 4 differentially regulate signaling via the G $\alpha_{q/11}$ -linked muscarinic M<sub>3</sub> receptor. *Mol Pharmacol* **66**:1453-1464.
- Vickers TA, Koo S, Bennett CF, Crooke ST, Dean NM, and Baker BF (2003) Efficient reduction of target RNAs by small interfering RNA and RNase H-dependent antisense agents. A comparative analysis. *J Biol Chem* **278**:7108-7118.
- Willems J, and Kelly E (2001) Desensitization of endogenously expressed  $\delta$ -opioid receptors: no evidence for involvement of G protein-coupled receptor kinase 2. *Eur J Pharmacol* **431**:133-141.
- Young KW, Nash MS, Challiss RAJ, and Nahorski SR (2003) Role of Ca<sup>2+</sup> feedback on single cell inositol 1,4,5-trisphosphate oscillations mediated by G-protein-coupled receptors. *J Biol Chem* **278**:20753-20760.
- Young SH, Wu SV, and Rozengurt E (2002) Ca<sup>2+</sup>-stimulated Ca<sup>2+</sup> oscillations produced by the Ca<sup>2+</sup>-sensing receptor require negative feedback by protein kinase C. *J Biol Chem* **277**:46871-46876.

MOL Manuscript # 14258

**Funding footnote:** This work was supported by the Wellcome Trust of Great Britain (Grant No. 062495), and a joint Biotechnology and Biological Sciences Research Council and GlaxoSmithKline PhD studentship to P.J.A.

**Address correspondence to:** Dr. R.A.J. Challiss, Department of Cell Physiology & Pharmacology, Maurice Shock Medical Sciences Building, University of Leicester, University Road, Leicester, LE1 9HN, UK. E-mail: [jc36@leicester.ac.uk](mailto:jc36@leicester.ac.uk)

## Figure Legends

**Fig. 1.** RNAi-mediated knockdown of  $G_{q/11}\alpha$  protein expression and function in HEK cells stably expressing the  $M_3$  mACh receptor. The initial identification of an active  $G_{q/11}\alpha$ -RNAi construct was carried out in HEK cells transiently transfected (using Lipofectamine 2000) with control RNAi or  $G_{q/11}\alpha$ -RNAi 72 h prior to experimentation, as described in Materials and Methods. Panel **A**, representative immunoblot demonstrating reduction of  $G_{q/11}\alpha$  protein expression relative to control RNAi-transfected HEK cell lysates. Equal amounts of each sample were loaded in duplicate and also probed for  $G_{i1-3}\alpha$  and  $\gamma$ -tubulin as a control for protein loading. Panel **B**, effects of  $G_{q/11}\alpha$ -RNAi on  $M_3$  mACh receptor function. Cells transfected (using GeneJuice) with eGFP-PH<sub>PLC $\delta$</sub>  alone (39 cells) and in combination with  $G_{q/11}\alpha$ -RNAi (26 cells) or control RNAi (28 cells) were challenged for 30 s with increasing concentrations of methacholine. Cells were washed with KHB for 180 s between each addition. The peak changes in cytosolic eGFP-PH<sub>PLC $\delta$</sub>  fluorescence were measured for each cell, and the data averaged (mean  $\pm$  S.E.M.) from at least 3 different experiments. Correlation coefficients of curve fits for eGFP-PH<sub>PLC $\delta$</sub>  alone, and in combination with  $G_{q/11}\alpha$ -RNAi or control RNAi were 0.99, 0.99 and 1.0, respectively. Representative images show the effect of  $G_{q/11}\alpha$  protein knockdown on single cell IP<sub>3</sub> production at a maximal concentration of methacholine.

**Fig. 2.** RNAi-induced knockdown of  $G_{q/11}\alpha$  protein expression in CHO cells. To assess the activity of the  $G_{q/11}\alpha$ -RNAi construct for use in CHO cell lines (where  $G_q\alpha$  and  $G_{11}\alpha$  sequence information was not available) stably expressing mGlu1 and mGlu5 receptors, cells were transfected (using GeneJuice) with control RNAi or  $G_{q/11}\alpha$ -RNAi 72 h prior to experimentation, as described in the Materials and Methods. Panel **A**, representative immunoblot showing reduction of  $G_{q/11}\alpha$  protein expression relative to control RNAi transfected CHO cell lysates. Equal amounts of each sample were loaded in duplicate as indicated following probing for  $G_{i1-3}\alpha$ ,  $G_{12}\alpha$  and  $\gamma$ -tubulin. Panel **B**, representative immunoblot showing the induction of mGlu1 and mGlu5 receptor expression by 100  $\mu$ M IPTG in control RNAi and  $G_{q/11}\alpha$ -RNAi transfected cells. Data are representative of at least three separate transfections.

**Fig. 3.** Determining the specificity of  $G_{q/11}\alpha$ -RNAi-mediated knockdown of  $G_q\alpha$  and  $G_{11}\alpha$  mRNA and protein expression in CHO cells. Panel **A**, sequencing  $G_q\alpha$  and  $G_{11}\alpha$  PCR products amplified from CHO cells. Following the identification of an RNAi construct with  $G_{q/11}\alpha$  silencing activity in both human and CHO cell backgrounds, the 19 base pair RNAi target sequence within  $G_q\alpha$  and  $G_{11}\alpha$  derived from the CHO cell line was confirmed. This region was amplified from CHO cells by PCR with  $G_q\alpha$  and  $G_{11}\alpha$  selective primers, based on rat sequence information (see Table 1). Shown is an alignment of the  $G_q\alpha$  and  $G_{11}\alpha$  PCR products from CHO cells with the equivalent human sequences to which the  $G_{q/11}\alpha$ -RNAi construct was targeted. Panel **B**, quantitative real-time PCR analysis of  $G_q\alpha$  and  $G_{11}\alpha$  mRNA following  $G_{q/11}\alpha$ -RNAi transfection into CHO-*lac*-mGlu1 and -mGlu5 cells. Data are expressed as % of control after normalization to cyclophilin (mean  $\pm$  S.E.M., \* $p$ <0.05 compared to control). All measurements were performed in triplicate following three separate transfections using the Amaxa Nucleofection system. Panel **C**, determining the relative knockdown of  $G_q\alpha$  and  $G_{11}\alpha$  protein expression levels following  $G_{q/11}\alpha$ -RNAi transfection. Lysates from the same transfected cells described in panel B were resolved by SDS-PAGE using a gel system containing 6 M urea to allow separation of  $G_q\alpha$  from  $G_{11}\alpha$  (see Materials and Methods). Immunodetection was carried out using antiserum CQ recognizing the conserved C-terminal region of both protein subunits. Shown are representative immunoblots, repeated at least three times, for (blot on *left*)  $\pm$   $G_{q/11}\alpha$ -RNAi effects, and (blot on *right*)  $G_q\alpha$  or  $G_{11}\alpha$  over-expression in CHO-*lac*-mGlu cells.

**Fig. 4.** Effect of  $G_{q/11}\alpha$  protein manipulation on the cell-surface expression of mGlu1a and mGlu5a receptors. CHO-*lac*-mGlu1a (**A**) or CHO-*lac*-mGlu5a (**B**) cells were transiently transfected with  $G_{q/11}\alpha$ -RNAi, control-RNAi or full-length human  $G_q\alpha$  cDNA using the Amaxa Nucleofection system (see Materials and Methods) 72 h prior to experimentation. Shown are representative immunoblots from three experiments indicating  $G_{q/11}\alpha$  protein and mGlu1a (A) or mGlu5a (B) receptor immunoreactivity using whole cell lysates, or following treatment of intact cell monolayers to biotinylate selectively cell-surface proteins.

**Fig. 5.** The effect of  $G_{q/11}\alpha$  protein manipulation on single cell  $IP_3$  responses in CHO-*lac*-mGlu1a cells. Cells co-transfected according to Materials and Methods, with eGFP-PH<sub>PLC $\delta$</sub>  and  $G_{q/11}\alpha$ -RNAi (n=18 cells), control RNAi (n=23 cells) or full length  $G_q\alpha$  (n=19 cells) were

challenged for 30 s with increasing concentrations of glutamate. Cells were washed with KHB for 180 s between each addition. The peak changes in cytosolic eGFP-PH<sub>PLC $\delta$</sub>  fluorescence were measured for each cell and the data averaged (mean  $\pm$  S.E.M.) for separate cells from at least 3 different experiments. Representative images show the effect of RNAi-mediated knockdown of G<sub>q/11</sub> $\alpha$  protein on mGlu1a receptor mediated single cell IP<sub>3</sub> production, using a maximal concentration of glutamate. Correlation coefficients of curve fits for G<sub>q/11</sub> $\alpha$ -RNAi, control and full-length G<sub>q</sub> $\alpha$  transfected cells were 0.77, 0.95 and 1.0, respectively.

**Fig. 6.** The effect of G<sub>q/11</sub> $\alpha$  protein manipulation on the temporal profile of single cell IP<sub>3</sub> responses in CHO-*lac*-mGlu5a cells. Cells were co-transfected with eGFP-PH<sub>PLC $\delta$</sub>  and G<sub>q/11</sub> $\alpha$ -RNAi (n=15 cells), control RNAi (n=34 cells) or full length G<sub>q</sub> $\alpha$  (n=24 cells), 72 h prior to experimentation (see Materials and Methods). Due to the relatively small size of mGlu5a-receptor-mediated IP<sub>3</sub> responses at a single cell level, a single maximal concentration of glutamate (30  $\mu$ M) was perfused for 3 min allowing temporal changes in IP<sub>3</sub> production to be measured. Shown is a summary of responses taken from a total of 73 cells on three separate days (panel **A**). In several cells responses were nominal, so that changes in fluorescence were not detected and these are indicated as non-responders. Cells that exhibited a single initial increase in IP<sub>3</sub> are indicated as single-spike responses. Other responses were classified in accordance with the representative traces shown, where oscillatory and saturating IP<sub>3</sub> signals were recorded from control RNAi and G<sub>q</sub> $\alpha$ -expressing cells, respectively (panel **B**). Panel **C**, effect of changing G<sub>q/11</sub> $\alpha$  protein expression on peak IP<sub>3</sub> (mean  $\pm$  S.E.M. for all cells, including non-responders; \**p*<0.05 compared to control).

**Fig. 7.** Changes in G<sub>q/11</sub> $\alpha$  protein expression level alter the temporal profile of Ca<sup>2+</sup> signaling following group I mGlu receptor activation. CHO-*lac*-mGlu1a or mGlu5a cells co-transfected with eGFP and G<sub>q/11</sub> $\alpha$ -RNAi, control RNAi or full length G<sub>q</sub> $\alpha$  were loaded with fura-2AM, and single cell images of changes in intracellular free Ca<sup>2+</sup> concentration ([Ca<sup>2+</sup>]<sub>i</sub>) were measured from GFP-containing cells, using an inverted epifluorescence microscope (Materials and Methods). Each concentration of the agonist, glutamate, was applied for 200 s. Shown are representative traces taken from single mGlu1a (**A**) or mGlu5a (**B**) receptor-expressing CHO cells after each treatment. Following G<sub>q/11</sub> $\alpha$ -RNAi transfection, mGlu1a expressing cells were largely unable to maintain the peak and plateau responses typically displayed in control RNAi



MOL Manuscript # 14258

cells, and are therefore denoted as ‘non-saturating’ (**C**). In CHO-*lac*-mGlu5a cells over-expressing  $G_q\alpha$ ,  $Ca^{2+}$  elevations were often sustained instead of displaying the characteristic PKC-dependent oscillatory responses; these are indicated as ‘saturating’ responses (**D**). The  $Ca^{2+}$  signatures (classified according to the response achieved at 100  $\mu$ M glutamate) obtained from 34-82 cells for each condition in both cell lines over four separate experiments are summarized in histograms as shown (panels C+D).

**Fig. 8.** Manipulating  $G_{q/11}\alpha$  expression alters the agonist-concentration threshold for mGlu1a and mGlu5a receptor-mediated signaling. mGlu receptor-mediated  $Ca^{2+}$  responses from the same experiments described in Fig. 7, were further analyzed to determine onset of  $Ca^{2+}$  signaling events. Histograms indicate the number of mGlu1 (**A**) or mGlu5 (**B**) receptor-expressing cells (as a percentage of the total) that are responding for the first time.

MOL Manuscript # 14258

**Table 1. Oligonucleotides**

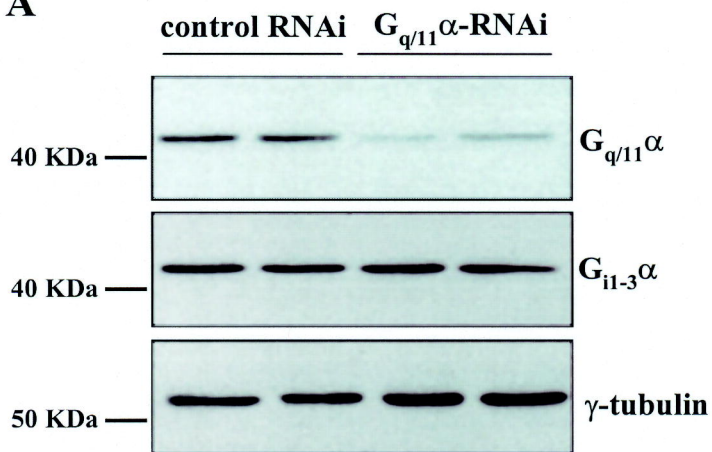
Gene	GenBank Accession Number	Primer	Sequence 5'-3'
<i>Rat</i>			
cyclophilin	<u>NM_017101</u>	s	TGTGCCAGGGTGGTGACTT
		as	CCACCAGTGCCATTATGGCGTGT
(For real-time PCR)			
G <sub>q</sub> α	<u>NM_031036</u>	s	AGTTCGAGTCCCCACCACAG
		as	CCTCCTACATCGACCATTCTGAA
G <sub>11</sub> α	<u>NM_031033</u>	s	GGTGGAGTCGGACAACGAGA
		as	GGGTAGGTGATGATTGTGCGG
(For sequencing)			
G <sub>q</sub> α	<u>NM_031036</u>	s	GGAGAAAATTATGTATTCC
		as	CTCCGTGTCTGTGGCACAC
G <sub>11</sub> α	<u>NM_031033</u>	s	AGACAAGATCCTGCACTCA
		as	TTCGGTGTCCGTGGCGCAG

Oligonucleotide sequences are shown for sense (s) and antisense (as) primers.

MOL Manuscript # 14258

# Figure 1

## A



## B

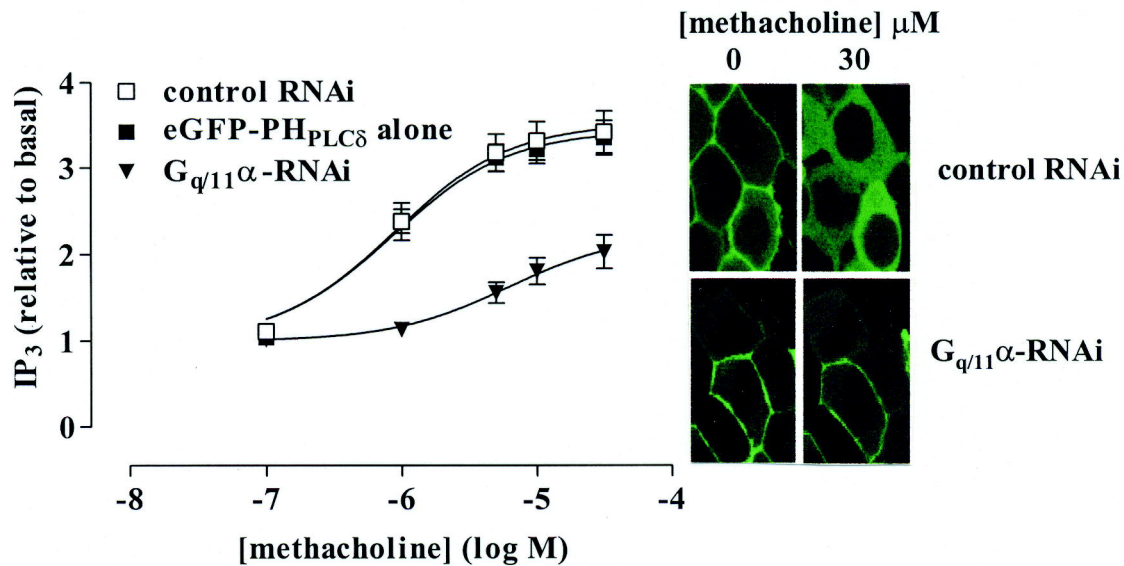


**Figure 2**

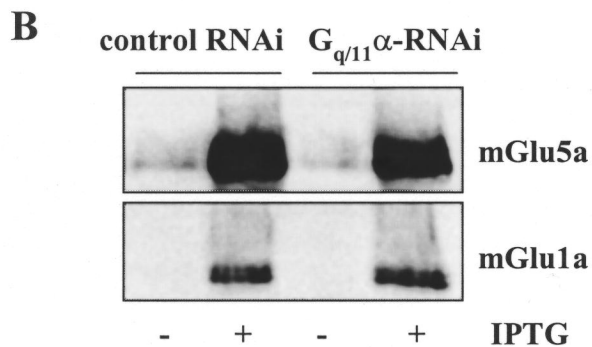
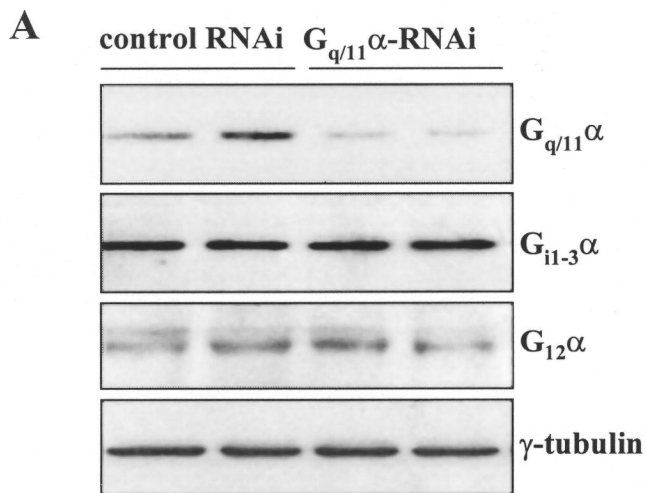
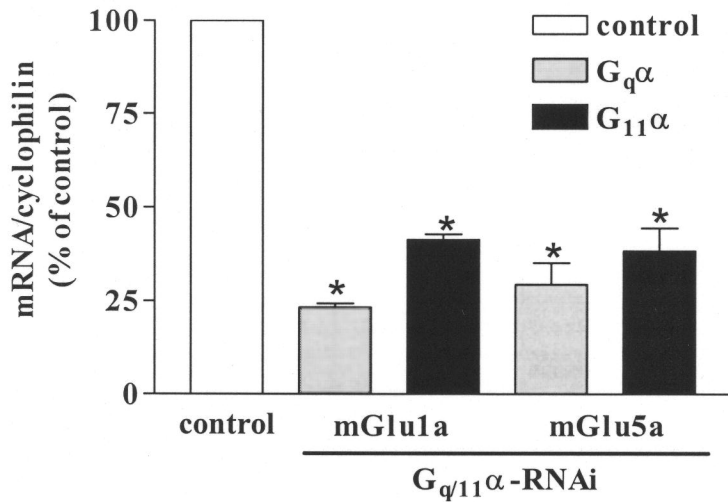


**Figure 3**

**A**

	1	2	3	4	5	6	7	8	9	10	11	12	13	14	15	16	17	18	19	20	21	
human $G_{q\alpha}$	A	A	G	A	T	G	T	T	C	G	T	G	G	A	C	C	T	G	A	A	C	
human $G_{11\alpha}$	A	A	G	A	T	G	T	T	C	G	T	G	G	A	C	C	T	G	A	A	C	
CHO $G_{q\alpha}$	A	A	G	A	T	G	T	T	C	G	T	G	G	A	C	C	T	G	A	A	C	
CHO $G_{11\alpha}$	A	A	G	A	T	G	T	T	<u>T</u>	C	G	T	G	G	A	C	C	T	G	A	<u>A</u>	<u>T</u>

**B**



**C**

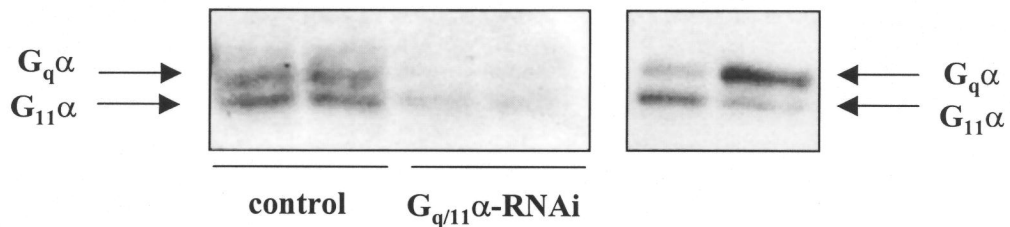


**Figure 4**

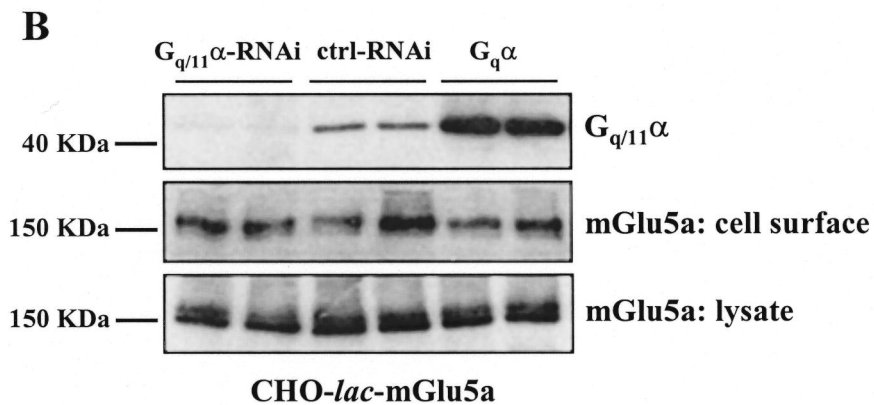
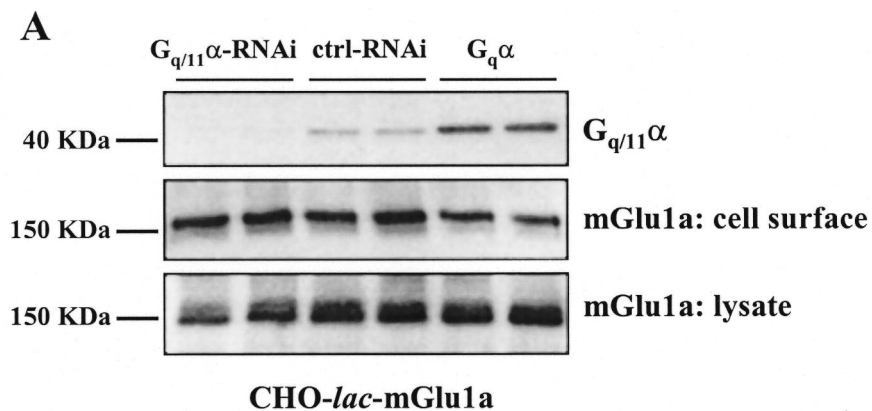


# Figure 5

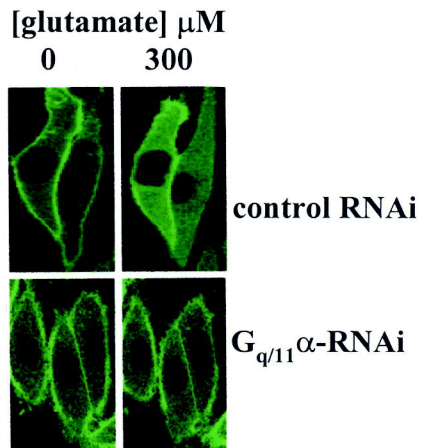
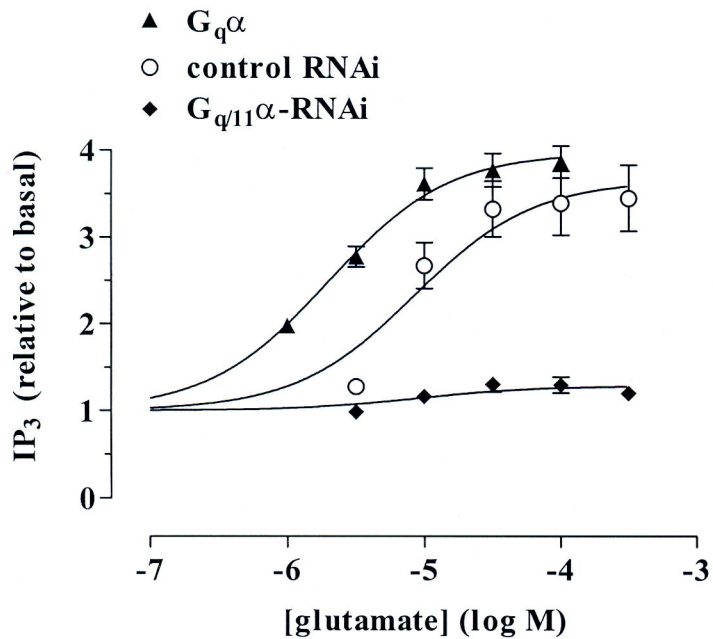
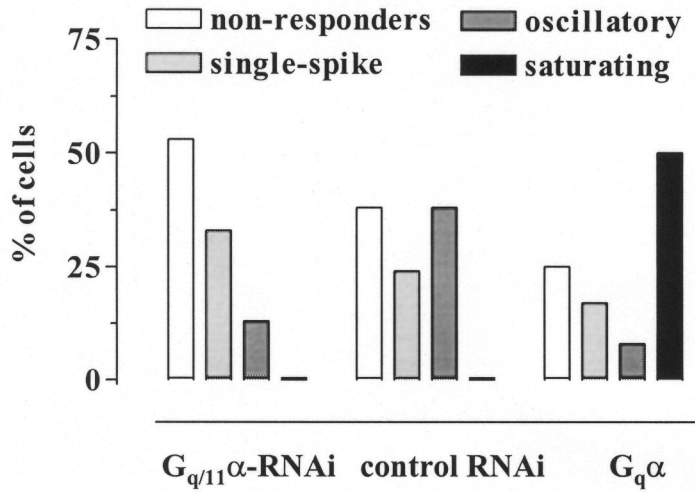


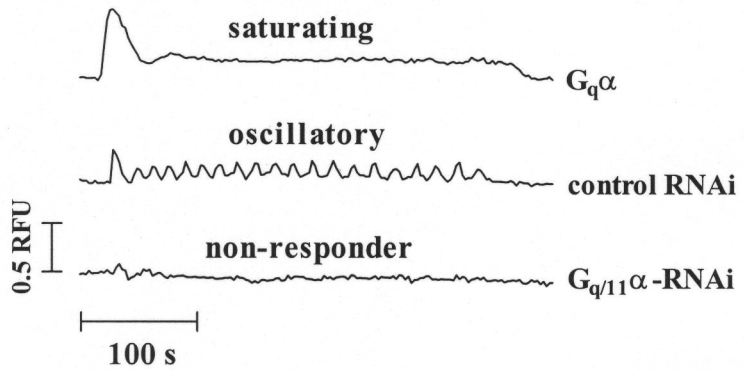


**Figure 6**

**A**



**B**



**C**

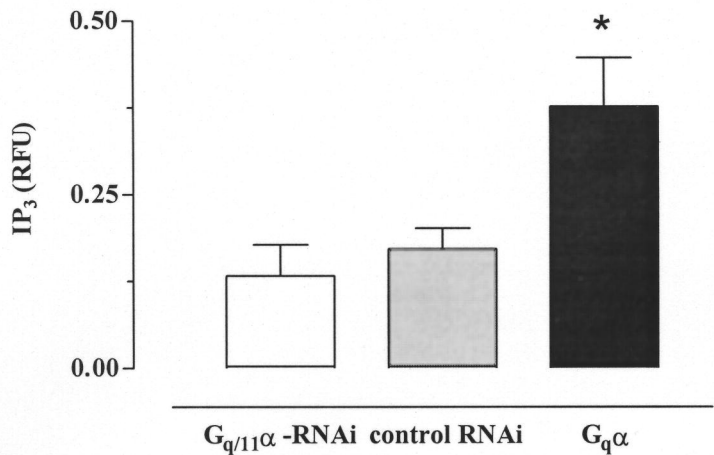


# Figure 7

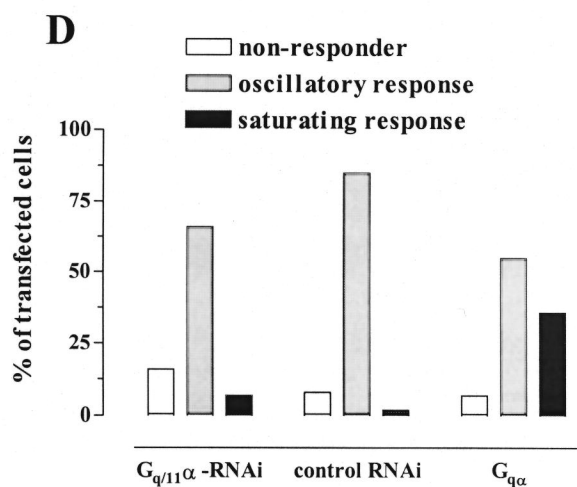
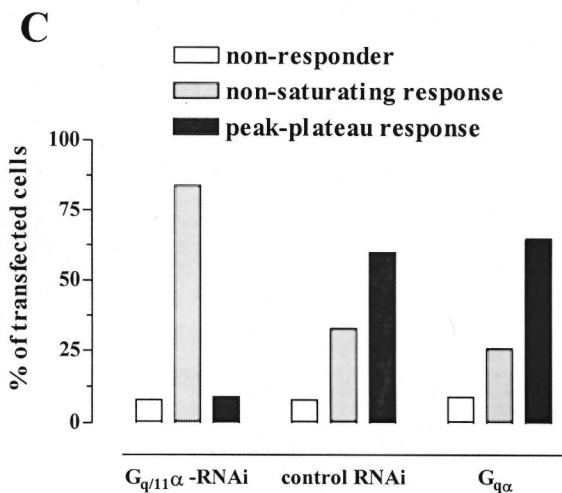
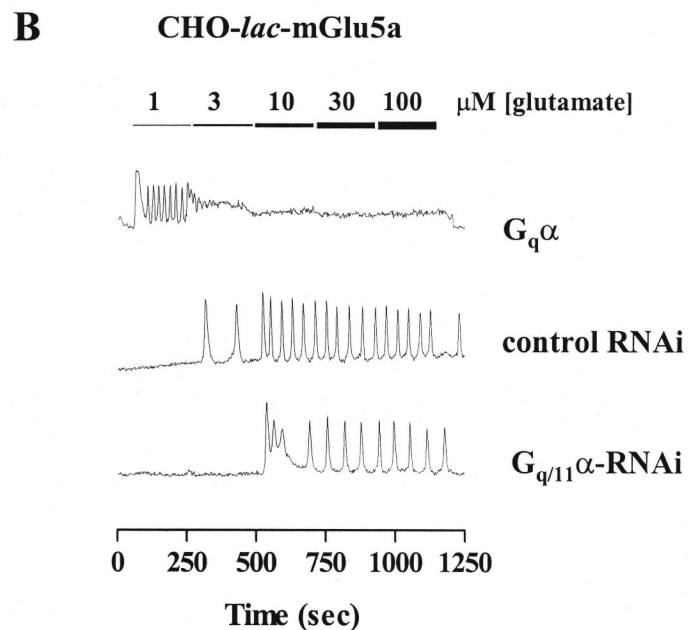
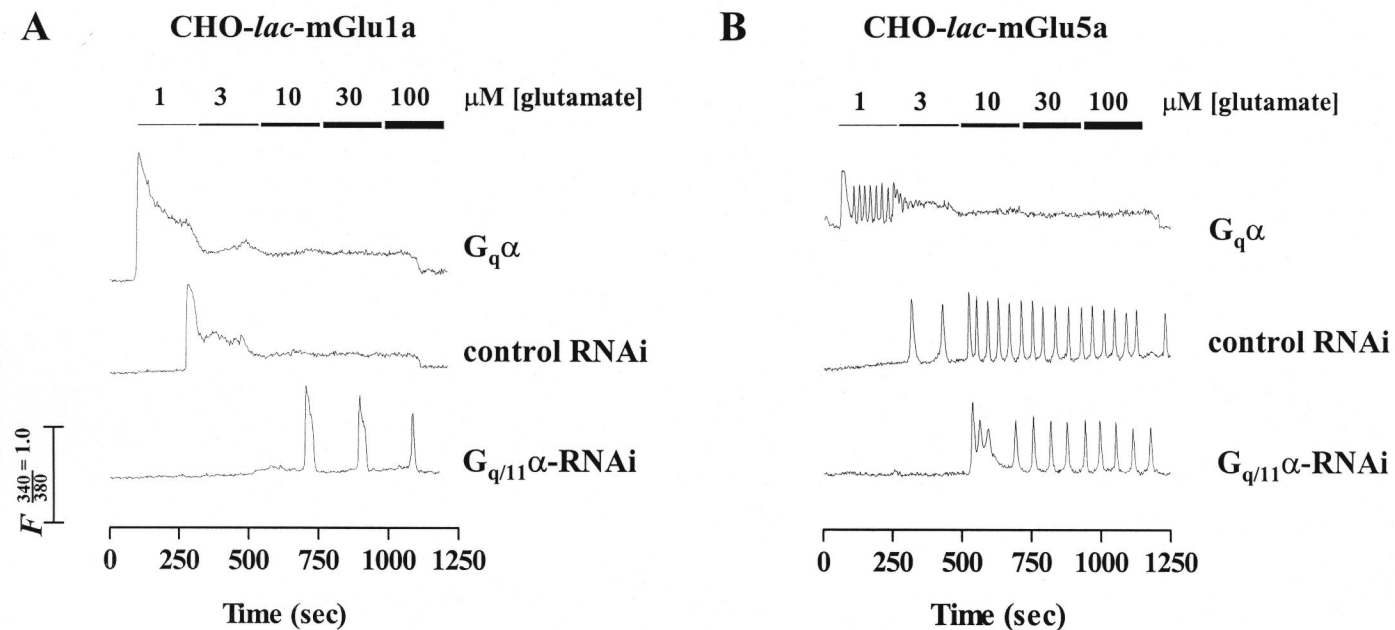


# Figure 8

